Carbohydrate Polymers 101 (2014) 650–655

Contents lists available at ScienceDirect

Carbohydrate Polymers

journal homepage: www.elsevier.com/locate/carbpol

Designing nanoemulsion templates for fabrication of dextrin nanoparticles via emulsion cross-linking technique

Somkamol Manchun[a,b], Crispin R. Dass[c,d,e], Pornsak Sriamornsak[a,b,*]

[a] Department of Pharmaceutical Technology, Faculty of Pharmacy, Silpakorn University, Nakhon Pathom 73000, Thailand
[b] Pharmaceutical Biopolymer Group (PBiG), Faculty of Pharmacy, Silpakorn University, Nakhon Pathom 73000, Thailand
[c] School of Pharmacy, Faculty of Health Sciences, Curtin University, Bentley 6102, Australia
[d] Curtin Health and Innovation Research Institute (CHIRI), Bentley 6102, Australia
[e] College of Health and Biomedicine, Victoria University, St Albans 3021, Australia

ARTICLE INFO

Article history:
Received 10 July 2013
Received in revised form 22 August 2013
Accepted 14 September 2013
Available online 23 September 2013

Keywords:
Dextrin
Nanoparticles
Emulsion crosslinking technique
Ultrasonication

ABSTRACT

The aim of this study was to prepare dextrin nanoparticles by emulsion cross-linking technique. The nanoparticles were prepared from nanoemulsion templates produced by high power ultrasonication. The influence of hydrophilic–lipophilic balance (HLB), surfactant type and concentration, water content, and sonication time on the template size were examined in order to find optimal conditions for preparing dextrin nanoparticles. Nano-scaled templates were achieved when mixed surfactants (Span80/Tween80 and Span80/Brij30) at HLB 6 were used while using Span80 or other HLB values resulted in micron-sized templates. The smallest emulsion templates were achieved when using 7% (w/w) mixture of Span80/Tween80 at HLB 6, 15% (w/w) water, and sonication time of 30 min. The spherical dextrin nanoparticles possessed a slight negative charge on the surface. FTIR spectra confirmed that dextrin was cross-linked by glyoxal. This study developed a novel way of formulating dextrin nanoparticles, which may prove to be useful in future for drug delivery.

1. Introduction

Currently, nanoparticles have been used in a wide number of applications, for example, as drug carriers, biosensors, and in the nanoelectronic field (Jiang, 2012; Qureshi, Kang, Davidson, & Gurbuz, 2009; Xie, Lee, & Chen, 2010). Due to their submicron size, nanoparticles possess a high surface-to-volume ratio, improved dispersibility and adaptability for multiple functions (Singh & Lillard, 2009). Both synthetic and natural materials have been investigated for fabrication of nanoparticles with different characteristics. Several natural biopolymers such as chitosan, alginate, pectin, polylactic acid, shellac, gelatin, starch and dextrin have received growing attention as nanocarriers for pharmaceutical applications. Dextrin, a saccharide-based polymer containing D-glucose units linked by α-(1 → 4) glycosidic bonds, is produced by partial hydrolysis of starch. It has a same general structure as starch but is smaller and thereby less complex (Carvalho, Gonçalves, Gil, & Gama, 2007). Dextrin is a widely used material with a variety of applications, from adhesives to food additives and textiles (Carvalho et al., 2007). Due to the biocompatibility and degradability attributes of dextrin, this biopolymer is used to prepare biodegradable drug carriers, especially hydrogels, with applications in a large number of areas such as medicine and pharmacy (Carvalho et al., 2007; Ferguson & Duncan, 2009).

Various techniques have been explored for the production of polysaccharide nanoparticles, including free radical graft polymerization, cross-linking by chemical reactions, radiation-induced polymerization and cross-linking, and self-assembly processes (Motornov, Roiter, Tokarev, & Minko, 2010). The emulsion (water-in-oil) cross-linking technique provides broad capabilities for variations in the structure that involves dispersion of an aqueous phase in an oil phase, in the presence of an effective surfactant system to produce nanoscale droplets or nanoemulsions (Burapapadh, Takeuchi, & Sriamornsak, 2012). The droplets of nanoemulsions can maintain the shape and size of the particles within the dispersed phase while generating starch particles through a cross-linking reaction (Ethirajan, Schoeller, Musyanovych, Ziener, & Landfester, 2008). Since the nanoemulsion is a non-equilibrium system, energy input from chemical potential or mechanical devices is required (Antonietti & Landfester, 2002; Landfester, 2001). Nanoemulsion can be prepared by high-energy emulsification methods or by low-energy emulsification methods (Noor El-Din & Al-Sabagh, 2012). Low-energy emulsification methods create chemical

* Corresponding author at: Department of Pharmaceutical Technology, Faculty of Pharmacy, Silpakorn University, Nakhon Pathom 73000, Thailand.
Tel.: +66 3425 5800; fax: +66 3425 5801.
E-mail addresses: pornsak@su.ac.th, spornsak@hotmail.com (P. Sriamornsak).

0144-8617/$ – see front matter © 2013 Elsevier Ltd. All rights reserved.
http://dx.doi.org/10.1016/j.carbpol.2013.09.049

potential through the use of surfactants. However, this method requires a large quantity of surfactants compared to the nanoemulsion which is obtained by the high-energy method (Liu, Sun, Li, Liu, & Xu, 2006). High-energy emulsification requires large mechanical energy generated by rotor–stator equipments such as ultrasound generator or high-pressure homogenizer to produce fine droplets (Lin & Chen, 2006; Burapapadh et al., 2012). The high-energy input provides forces that are able to deform and break off drops into smaller ones, provided the Laplace pressure is overcome. Adsorption of surfactant at the drop interface reduces the Laplace pressure (Solans et al., 2003), however, the smaller the droplet size, the higher the energy required for further drop break-off (Shi, Li, Wang, Li, & Adhikari, 2011).

Ultrasonic emulsification is a type of mechanical homogenizing technique that has been used for emulsion preparation by ultrasonic vibrating waves. Powerful ultrasonic waves with a high frequency can generate a continuous cycle of production and collapse of air bubbles, causing a phenomenon called cavitation. Large amounts of energy are released by this process and are transferred to the liquid solution, thereby creating a mechanical dispersion effect, which can result in homogeneous emulsification (Lin & Chen, 2006). It was found that the ultrasonic homogenizer creates emulsions with smaller droplet size and better stability than a simple homogenizer (Abismaïl, Canselier, Wilhelm, Delmas, & Gourdon, 1999). Moreover, the ultrasonic emulsification technique has been used to prepare emulsions for various applications including the food (Koocheki & Kadkhodaee, 2011) and fuel (Lin & Chen, 2006) industries.

The present study aimed to prepare dextrin nanoparticles using a two-step process. Firstly, nanoemulsion templates were prepared by high power ultrasonication. The effects of various parameters such as HLB, concentration of surfactant, water content and sonication time were investigated to optimize conditions that provide the smallest droplet size for fabrication of dextrin nanoparticles. Secondly, dextrin nanoparticles were produced using the emulsion cross-linking technique in the nanoemulsion templates. The physicochemical properties of the obtained dextrin nanoparticles were characterized.

2. Materials and methods

2.1. Materials

Dextrins (MW of 1400 and 1000, referred as D2 and D4, respectively) were donated by the Siam Modified Starch Co., Ltd. (Pathumthani, Thailand). Glyoxal and ethanol were obtained from Sigma–Aldrich Chemie (Steinheim, Germany). Hydrochloric acid and *n*-hexane were purchased from RCI Labscan (Bangkok, Thailand). Tween® 80, Brij® 30 and Span® 80 were purchased from PC Drug Center Co., Ltd. (Bangkok, Thailand) and are hereafter referred to as Tween80, Brij30 and Span80, respectively. All reagents were of analytical grade or pharmaceutical grade and used as supplied without further purification. Deionized water was used throughout the study.

2.2. Preparation of nanoemulsion templates

Nanoemulsion templates were prepared by a high energy emulsification method using high power ultrasonicator (400 W, 24 KHz) with constant amplitude (100%). A water bath was also used to maintain the temperature of the mixture at $30 \pm 2\,^{\circ}C$. In this method, different amounts of water were added to the *n*-hexane phase containing a mixture of Span80 and Tween80 or Brij30 at various ratios.

2.3. Preparation of dextrin nanoparticles

To prepare dextrin nanoparticles, dextrin was dissolved in the water phase to obtain the final concentration of 5% (w/w) and then added to the emulsions obtained from Section 2.2. The mixture was ultrasonicated for 1 min to form nanoemulsions. After the nanoemulsion was formed, glyoxal (as a cross-linker) was added immediately and ultasonicated for 30 min. The obtained mixtures were then stirred with a magnetic stirrer for 12 h to continue the cross-linking reaction. The dextrin nanoparticles were precipitated from the nanoemulsion by adding 99% ethanol and washed 3 times with ethanol and finally rinsed with deionized water. Subsequently, the nanoparticles were dried by lyophilization for 24 h. The dry nanoparticles obtained from the lyophilization process was kept in a plastic bag and stored in the refrigerator (4–5 °C) until further use.

2.4. Droplet size and surface charge (zeta potential)

The mean droplet size and surface charge of the prepared nanoemulsions were determined using a laser scattering particle size distribution analyzer (model LA-950, Horiba, Japan) and zeta potential analyzer (Zeta Plus, Brookhaven, USA), respectively. The measurement of particle size and surface charge was performed in triplicate.

2.5. Morphology

Surface morphology of dextrin nanoparticles was observed using scanning electron microscope (SEM; model Maxim-2000, Camscan Analytical, England) and transmission electron microscopy (TEM; model JEM-1230, JOEL Corp., Japan). SEM samples were sputter-coated with gold to increase their conductance. The samples are then viewed and photographed using SEM. TEM analyses were performed by sample mounting on a copper glider grid of 3.5 mm with a single aperture.

2.6. FT-IR spectroscopic analysis

The prepared nanoparticles were blended with KBr and compressed at a pressure of 5 tons for 30 s. The KBr discs were scanned by FTIR spectrophotometer (Nicolet 4700, USA) in a range of 4000–400 cm^{-1}.

2.7. Statistical analysis

Analysis of variance (ANOVA) was performed using SPSS version 11.5 for Windows (SPSS Inc., USA). *Post hoc* testing ($p < 0.05$) of the multiple comparisons was performed by either the Scheffé or Games-Howell test depending on whether Levene's test was insignificant or significant, respectively.

3. Results and discussion

3.1. Formation of nanoemulsion templates

In this study, water-in-hexane emulsions were formed by high energy emulsification technique using high power (400 W, 24 KHz) ultrasonication. Generally, the emulsion droplet formed by high energy emulsification method is controlled by the interplay between droplet break up and droplet coalescence (Dickinson, 2003; McClements, 2004). Moreover, droplet break up is controlled by the type and amount of shear applied to the droplets as well as the droplets' resistance to deformation which is determined by the surfactant. The rate of droplet coalescence is determined by the ability of the surfactant to adsorb on to the surface of newly formed droplets; this is governed by the surfactant concentration and the

surface activity (Burapapadh, Kumpugdee-Vollrath, Chantasart, & Sriamornsak, 2010; McClements, 2004). The adsorbed surfactant causes a lowering in interfacial tension for easier emulsification and stabilizes the droplet against coalescence by steric or electrostatic repulsion (Noor El-Din & Al-Sabagh, 2012).

3.2. Effect of variables on droplet size of nanoemulsion templates

3.2.1. Effect of HLB

The chemical structure of emulsifier molecules at the interface of emulsion droplets is an important determinant of the stability and physical properties of obtained nanoemulsions. In this study, non-ionic surfactants consisting of both hydrophilic and lipophilic functional groups were used as emulsifier to form the nanoemulsion template. To optimize non-ionic surfactant efficiency in the nanoemulsion template preparation, the HLB system was used. The concept of HLB was established by Griffin (1949), and can be used to characterize the relative affinity of surfactant for aqueous and oil phases. According to Griffin's classification, a surfactant that is lipophilic in character is assigned a low HLB number and a surfactant that is hydrophilic in character is assigned a high number (Jin, Streett, Dunlap, & Lyn, 2008). Usually, a stable w/o emulsion requires the HLB number to fall within 8–13. In the present study, the nanoemulsion templates were prepared using various types of non-ionic surfactants – Tween80, Brij30 and Span80. The mixing ratio was adjusted to obtain the proper HLB values for suitable emulsification conditions. The mixed HLB values (HLB value of blended emulsifiers) were calculated using Eq. (1):

$$\mathrm{HLB_{mix}} = \mathrm{HLB}_x x\% + \mathrm{HLB}_y y\% \quad (1)$$

where x and y are low HLB surfactant and high HLB surfactant respectively, $x\%$ and $y\%$ are the mass percentage of high HLB surfactant and low HLB surfactant respectively, and where all the HLB values used were obtained at 25 °C.

The effect of HLB values on size of emulsions using Span80 (HLB = 4.3), mixture of Span80 and Tween80 (HLB = 15) and mixture of Span80 and Brij30 (HLB = 9.7) with different ratios to give HLB = 4.3, 6, 8, and 10, as shown in Fig. 1a. Nano-sized droplets were obtained at HLB = 6 with Span80 and Tween80, which allowed a minimum droplet size to be achieved. The droplet size of emulsions prepared by using mixed surfactant with HLB values greater than 6 was larger. The emulsions using only Span80 (HLB = 4.3) exhibited a maximum droplet size (4.67 μm). These findings suggested that the formation of minimum droplet is independent on HLB number. With suitable HLB value, the surfactants are allowed to partition between hexane and aqueous phases, resulting in lower interfacial tension and smaller droplet size.

3.2.2. Effect of concentration and type of surfactant

A significant decrease in droplet size was found when the concentration of surfactant in the formulation was increased (Fig. 1b). The relationship between emulsion droplet size and surfactant concentration can be explained in terms of surfactant surface coverage ability. At low concentrations of surfactant, there is insufficient surfactant to completely adsorb and cover the entire surface of hexane droplets during the homogenization process (Shi et al., 2011). The increase of surfactant concentration, however, resulted in a large decrease in droplet size because more surfactant was available to allow rapid diffusion and adsorption on newly formed droplets. According to thermodynamic approach, increasing concentration of surfactant, resulting in rapid adsorption kinetics and favorable adsorption equilibria, is most effective in reducing the interfacial tension and stabilizing newly formed droplets (Maindarkar, Bongers, & Henson, 2013). Furthermore, using mixed surfactant also reduced interfacial tension by their synergistic effect (Razavizadeh et al., 2004).

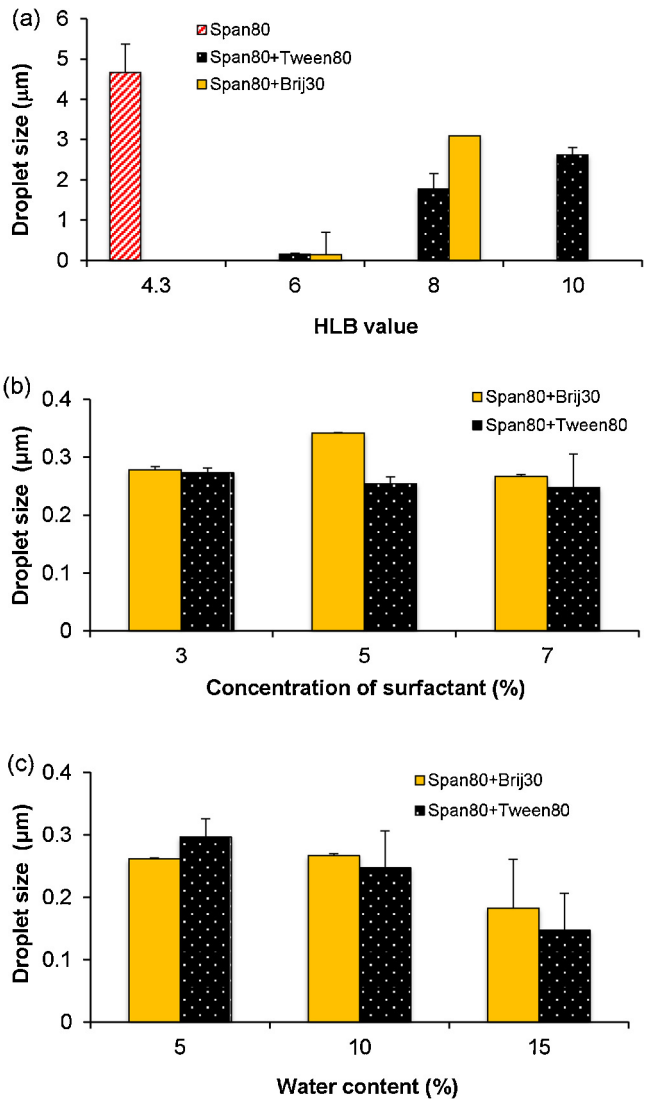

Fig. 1. Droplet size of nanoemulsions prepared by ultrasonication for 10 min; (a) effect of HLB on droplet size of emulsions prepared using water content and surfactant concentration of 10% and 5% respectively, (b) effect of surfactant concentration on droplet size of emulsions prepared by using a mixture of surfactant at HLB = 6 and water content of 10%, and (c) effect of water content on droplet size of emulsions prepared by using a mixture of surfactant at HLB = 6 and surfactant concentration of 7%.

From Fig. 1, it is obvious that not only the concentration of surfactant but also the type of mixed surfactant influenced the size of emulsion droplets. Inclusion of Span80/Brij30 in the formulation showed larger droplet size, ranged from 267 to 342 nm. In contrast, addition of Span80/Tween80 in the formulation yielded emulsions with smaller droplet size, about 214–277 nm. According to the chemical structure of surfactant, Tween80 has a branched hydrophilic head group, namely ethylene oxide, spread between the branches, resulting in a larger surface area to interact with water whereas Brij30, a smaller and shorter molecule having a straight chain structure, has limited surface area for interaction with the dispersed phase. Moreover, the chemical structure of Tween80 is similar to Span80 with the same hydrocarbon chain length, that is, an oleate chain with 18 carbon atoms and one unsaturated bond. This leads to a synergistic effect in the dispersion of water in w/o nanoemulsions, providing better states of minimum energy and a more stable interface (Huibers & Shah, 1997).

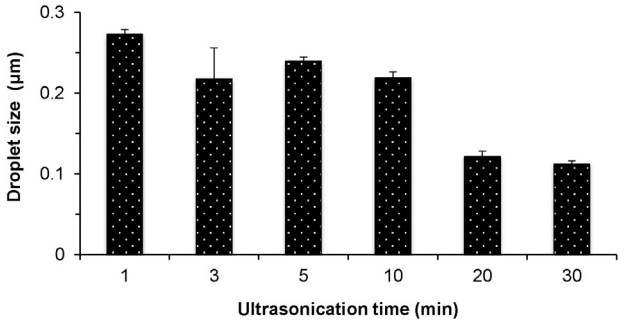

Fig. 2. Effect of sonication time on droplet size of emulsions prepared using different ultrasonication times. The HLB of a mixture of Span80/Tween80 was fixed at 6, the surfactant concentration was 7%, and the water content was 15%.

3.2.3. *Effect of water content*

The droplet size in water-in-hexane emulsion using mixed surfactant at HLB value of 6 with different water contents (5, 10, and 15% w/w) is shown in Fig. 1c. From the results, it is apparent that the droplet size significantly decreased with the increased water content. Similar results regarding the effect of the dispersed phase fraction on particle size was examined in an earlier study (Cho & Kamal, 2002). It is thought that the deformation rate increased with rising volume fractions of the dispersed phase and high shear stress, leading to an increase in droplet breakup. The total deformation of the dispersed phase increased with increasing volume fractions, resulting in the droplet size of the dispersed phase being decreased (Cho & Kamal, 2002). Therefore, using high power ultrasonication, which possesses high shear stress, and increasing water content could lead to a decrease in the droplet size of the emulsion template. Moreover, using Span80/Tween80 in the formulation provided emulsions with a smaller droplet size.

3.2.4. *Effect of ultrasonication time*

In this study, the nanoemulsion templates were prepared by a high intensity probe ultrasonicator (ultrasound power of 400 W, 24 KHz). For this, a diphasic liquid system is treated by high-frequency vibrations of ultrasound power to provide a different phenomenon of breaking and dispersing in a bulk phase, resulting in large droplets being broken into smaller ones by acoustic cavitation (Abismaïl et al., 1999). The effect of ultrasonication time on the droplet size was investigated by varying the ultrasonication time from 1 to 30 min (Fig. 2). Increasing sonication time decreased the droplet size of the nanoemulsion templates. Gaikwad and Pandit (2008) reported that increasing the sonication time raises the temperature of the emulsion. It is thought that the increase in temperature results in an increase in the vapour pressure of the cavitating medium, leading to an increase in the number of nuclei which give rise to cavitation. As a result of the increase in the cavitational events, breaking of large droplets to form smaller ones occurs (Gaikwad & Pandit, 2008). However, no significant difference was found between droplet sizes of nanoemulsion templates obtained when using ultrasonication time over a 10-min period. Energy supplied over a longer period of time (20–30 min) led to smaller droplet sizes (>50% reduction in size).

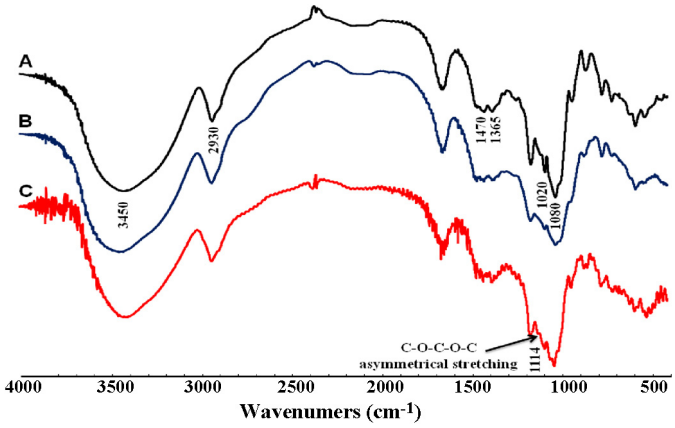

Fig. 4. FTIR spectra of (A) native dextrin (MW of 1400), (B) physical mixture of dextrin and glyoxal (1:1), and (C) dextrin nanoparticles.

3.3. *Preparation of dextrin nanoparticles*

Dextrin nanoparticles were fabricated in water-in-hexane nanoemulsion templates using an emulsion cross-linking technique with glyoxal as the cross-linker. The composition and ratio of the water and hexane phases are shown in Table 1. Glyoxal is a dialdehyde compound that has been used as cross-linking agent for various polymers, including chitosan (Gupta & Jabrail, 2006; Wang & Stegemann, 2011; Yang, Dou, Liang, & Shen, 2005), starch (Uslu & Polat, 2012), cellulose (Yanagida & Matsuo, 1992) and polyvinyl alcohol (Qiu & Netravali, 2012). In the present study, the hydroxyl groups of dextrin molecules reacted with glyoxal to create three-dimensional structures in the form of nanoparticles. An overview of the chemical reaction between glyoxal and dextrin is presented in Fig. 3. The carbonyl group of aldehyde can react with a hydroxyl group by nucleophilic addition to form a hemiacetal compound (Solomons, 1980). Being unstable in nature, this compound reacts readily with another hydroxyl group again to form an acetal linkage.

From the FTIR spectrum of native dextrin (Fig. 4), a broad peak was noted at 3450 cm^{-1} due to the stretching vibrations of O—H, a small peak at 2930 cm^{-1} attributed to the C—H stretching vibrations, 1365–1470 cm^{-1} for C—H bending, and 1020–1080 cm^{-1} for C—O stretching. For dextrin nanoparticles after the crosslinking reaction, a new peak of C—O—C—O—C asymmetrical stretching

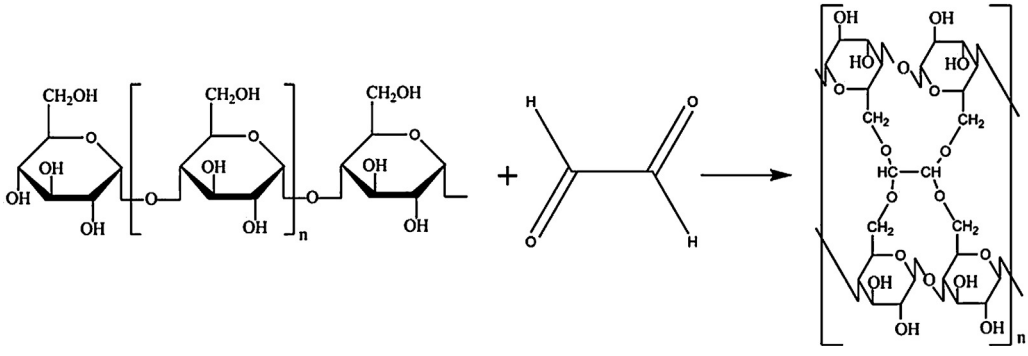

Fig. 3. Mechanism of cross-linking reaction. Dextrin chains are chemically bonded with glyoxal, resulting in a cross-linked dextrin chain.

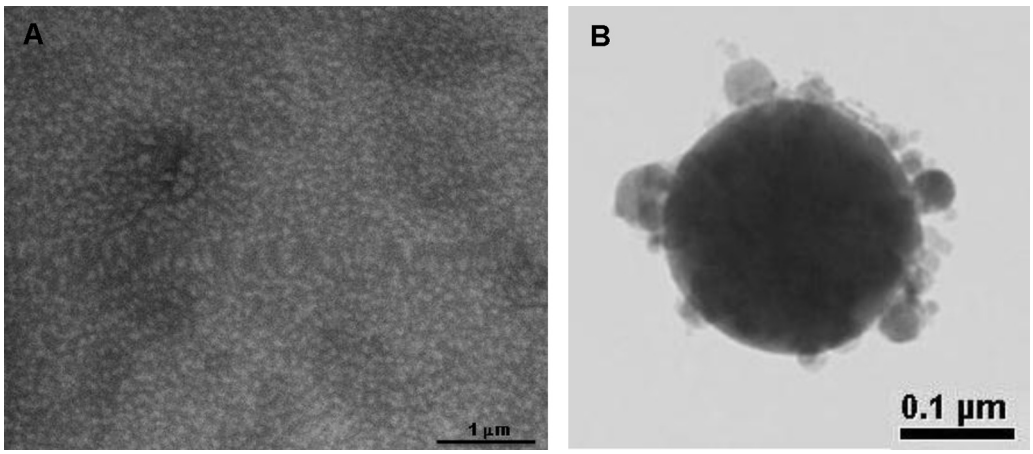

Fig. 5. Morphology of dextrin (D2) nanoparticles prepared from nanoemulsion templates as observed by (A) SEM and (B) TEM.

Table 1
Composition and ratio of the constituents in water phase and hexane phase.

	Dextrin (%)	Glyoxal (mL)	*n*-Hexane (g)	Surfactant (g)	Distilled water (g)
Water phase	5	0.12	0	0	9.88
Hexane phase	0	0	78	7	0

Table 2
Physical properties of prepared dextrin nanoparticles.

Type of dextrin	Particle size (nm)	ζ-Potential (mV)
D2	0.123 ± 0.014	−5.067 ± 0.7
D4	0.206 ± 0.015	−5.260 ± 3.4

appeared at 1114 cm^{-1} but was not observed with physical mixture. This indicated that glyoxal has reacted with the hydroxyl groups of dextrin due to acetalization. The results were consistent with a previous work by Yang, Dou, Liang, and Shen (2005).

The average size and the ζ-potential of dextrin nanoparticles are given in Table 2. Different results were obtained with the two different molecular weights of dextrin, 1000 (D4) and 1400 (D2). The smallest size was achieved when the higher molecular weight dextrin (D2) was used. It is possible that the higher molecular weight dextrin containing a larger quantity of hydroxyl groups had more interactions with glyoxal and led to an increase in the cross-linking density in the nanoemulsion template. The dextrin nanoparticles are spherical in shape (Fig. 5), with overlapping of the emulsion droplet on the surface during sample preparation, as the particles tend to aggregate together.

4. Conclusion

Dextrin nanoparticles were successfully produced by an emulsion cross-linking technique using glyoxal as a cross-linker. The results demonstrated that sonication time, value of HLB, amount of water, type and amount of surfactant in formulation were critical determinants of template size. The droplet size of emulsion templates decreased as a factor of increased surfactant concentration, water content and sonication time. With judicious manipulations of these parameters, namely using 7% (w/w) mixture of Span 80/Tween80 at HLB 6, 15% (w/w) water and sonication time of 30 min, the smallest nanoemulsion templates were obtained. The obtained dextrin nanoparticles displayed spherical shape and slightly negative charge on the surface. This study demonstrated a new method to develop dextrin nanoparticles from nanoemulsion templates prepared by high power ultrasonication. These dextrin nanoparticles may serve as an effective “nanocarrier” for the formulation of poorly water-soluble drugs by increasing their water solubility, improving their stability, and controlling their release profile. Also, incorporation of anticancer drugs into dextrin nanoparticles may be advantageous for passive targeting of tumor tissues, after intravenous administration.

Acknowledgments

The authors wish to acknowledge The Thailand Research Fund for the financial support (grant number BRG5480013). SM is financially supported by the Royal Golden Jubilee Ph.D. Program (grant number PHD/0361/2551) and Curtin University Academic50 Scheme. Thanks also to Dr. Akamol Klaikherd who has inspired us to conduct this study, and Siam Modified Starch Co., Ltd. (Pathumthani, Thailand) who kindly supplied dextrin samples.

References

Abismaïl, B., Canselier, J. P., Wilhelm, A. M., Delmas, H., & Gourdon, C. (1999). Emulsification by ultrasound: Drop size distribution and stability. *Ultrasonics Sonochemistry*, *6*(1-2), 75–83.

Antonietti, M., & Landfester, K. (2002). Polyreactions in miniemulsions. *Progress in Polymer Science*, *27*(4), 689–757.

Burapapadh, K., Kumpugdee-Vollrath, M., Chantasart, D., & Sriamornsak, P. (2010). Fabrication of pectin-based nanoemulsions loaded with itraconazole for pharmaceutical application. *Carbohydrate Polymers*, *82*(2), 384–393.

Burapapadh, K., Takeuchi, H., & Sriamornsak, P. (2012). Novel pectin-based nanoparticles prepared from nanoemulsion templates for improving *in-vitro* dissolution and *in-vivo* absorption of poorly water-soluble drug. *European Journal of Pharmaceutics and Biopharmaceutics*, *82*(2), 250–261.

Carvalho, J., Gonçalves, C., Gil, A. M., & Gama, F. M. (2007). Production and characterization of a new dextrin based hydrogel. *European Polymer Journal*, *43*(7), 3050–3059.

Cho, Y. G., & Kamal, M. R. (2002). Effect of the dispersed phase fraction on particle size in blends with high viscosity ratio. *Polymer Engineering & Science*, *42*(10), 2005–2015.

Dickinson, E. (2003). Hydrocolloids at interfaces and the influence on the properties of dispersed systems. *Food Hydrocolloids*, *17*(1), 25–39.

Ethirajan, A., Schoeller, K., Musyanovych, A., Ziener, U., & Landfester, K. (2008). Synthesis and optimization of gelatin nanoparticles using the miniemulsion process. *Biomacromolecules*, *9*(9), 2383–2389.

Ferguson, E. L., & Duncan, R. (2009). Dextrin-phospholipase A2: Synthesis and evaluation as a bioresponsive anticancer conjugate. *Biomacromolecules*, *10*(6), 1358–1364.

Gaikwad, S. G., & Pandit, A. B. (2008). Ultrasound emulsification: Effect of ultrasonic and physicochemical properties on dispersed phase volume and droplet size. *Ultrasonics Sonochemistry*, *15*(4), 554–563.

Griffin, W. C. (1949). Classification of surface-active agents by 'HLB'. *Journal of the Society of Cosmetic Chemists*, *1*, 311.
Gupta, K. C., & Jabrail, F. H. (2006). Glutaraldehyde and glyoxal cross-linked chitosan microspheres for controlled delivery of centchroman. *Carbohydrate Research*, *341*(6), 744–756.
Huibers, P. D. T., & Shah, D. O. (1997). Evidence for synergism in nonionic surfactant mixtures: Enhancement of solubilization in water-in-oil microemulsions. *Langmuir*, *13*, 5762–5765.
Jiang, S. P. (2012). Nanoscale and nano-structured electrodes of solid oxide fuel cells by infiltration: Advances and challenges. *International Journal of Hydrogen Energy*, *37*(1), 449–470.
Jin, X., Streett, D. A., Dunlap, C. A., & Lyn, M. E. (2008). Application of hydrophilic–lipophilic balance (HLB) number to optimize a compatible nonionic surfactant for dried aerial conidia of *Beauveria bassiana*. *Biological Control*, *46*(2), 226–233.
Koocheki, A., & Kadkhodaee, R. (2011). Effect of *Alyssum homolocarpum* seed gum, Tween 80 and NaCl on droplets characteristics, flow properties and physical stability of ultrasonically prepared corn oil-in-water emulsions. *Food Hydrocolloids*, *25*(5), 1149–1157.
Landfester, K. (2001). Polyreactions in miniemulsions. *Macromolecular Rapid Communications*, *22*(12), 896–936.
Lin, C.-Y., & Chen, L.-W. (2006). Emulsification characteristics of three- and two-phase emulsions prepared by the ultrasonic emulsification method. *Fuel Processing Technology*, *87*(4), 309–317.
Liu, W., Sun, D., Li, C., Liu, Q., & Xu, J. (2006). Formation and stability of paraffin oil-in-water nano-emulsions prepared by the emulsion inversion point method. *Journal of Colloid and Interface Science*, *303*(2), 557–563.
Maindarkar, S. N., Bongers, P., & Henson, M. A. (2013). Predicting the effects of surfactant coverage on drop size distributions of homogenized emulsions. *Chemical Engineering Science*, *89*, 102–114.
McClements, D. J. (2004). *Food emulsions: Principles, practices, and techniques*. Florida: CRC Press.
Motornov, M., Roiter, Y., Tokarev, I., & Minko, S. (2010). Stimuli-responsive nanoparticles, nanogels and capsules for integrated multifunctional intelligent systems. *Progress in Polymer Science*, *35*(1-2), 174–211.
Noor El-Din, M. R., & Al-Sabagh, A. M. (2012). Preparation of water-in-hexane nanoemulsions using low energy emulsification method. *Journal of Dispersion Science and Technology*, *33*(1), 68–74.
Qiu, K., & Netravali, A. N. (2012). Fabrication and characterization of biodegradable composites based on microfibrillated cellulose and polyvinyl alcohol. *Composites Science and Technology*, *72*(13), 1588–1594.
Qureshi, A., Kang, W. P., Davidson, J. L., & Gurbuz, Y. (2009). Review on carbon-derived, solid-state, micro and nano sensors for electrochemical sensing applications. *Diamond and Related Materials*, *18*(12), 1401–1420.
Razavizadeh, B. M., Mousavi-Khoshdel, M., Gharibi, H., Behjatmanesh-Ardakani, R., Javadian, S., & Sohrabi, B. (2004). Thermodynamic studies of mixed ionic/nonionic surfactant systems. *Journal of Colloid and Interface Science*, *276*(1), 197–207.
Shi, A. M., Li, D., Wang, L. J., Li, B. Z., & Adhikari, B. (2011). Preparation of starch-based nanoparticles through high-pressure homogenization and miniemulsion cross-linking: Influence of various process parameters on particle size and stability. *Carbohydrate Polymers*, *83*(4), 1604–1610.
Singh, R., & Lillard, J. W., Jr. (2009). Nanoparticle-based targeted drug delivery. *Experimental and Molecular Pathology*, *86*(3), 215–223.
Solans, C., Esquena, J., Forgiarini, A. M., Ulson, N., Morales, D., Izquierdo, P., et al. (2003). *Absorption and aggregation of surfactants in solution*. New York: Marcel Dekker.
Solomons, T. W. G. (1980). *Organic chemical*. New York: Wiley.
Uslu, M., & Polat, S. (2012). Effects of glyoxal cross-linking on baked starch foam. *Carbohydrate Polymers*, *87*(3), 1994–1999.
Wang, L., & Stegemann, J. P. (2011). Glyoxal crosslinking of cell-seeded chitosan/collagen hydrogels for bone regeneration. *Acta Biomaterialia*, *7*(6), 2410–2417.
Xie, J., Lee, S., & Chen, X. (2010). Nanoparticle-based theranostic agents. *Advanced Drug Delivery Reviews*, *62*(11), 1064–1079.
Yanagida, N., & Matsuo, M. (1992). Morphology and mechanical properties of hydroxypropyl cellulose cast films crosslinked in solution. *Polymer*, *33*(5), 996–1005.
Yang, Q., Dou, F., Liang, B., & Shen, Q. (2005). Studies of cross-linking reaction on chitosan fiber with glyoxal. *Carbohydrate Polymers*, *59*(2), 205–210.